

EVOLUTION OF TEMPERATURE AND DAMAGE IN ROCK MASS AFTER HEAT SHOCK

by

**Xiao-Yan ZHU^{a,b}, Duo XU^{a,b}, Teng TENG^{a,b,c*}, Peng YI^{a,b},
Wen-Kang WANG^{a,b}, and Jia-Xin WANG^a**

^aState Key Laboratory for Geo-Mechanics and Deep Underground Engineering,
China University of Mining and Technology, Beijing, China

^bState Key Laboratory Cultivation Base for Gas Geology and Gas Control,
Henan Polytechnic University, Jiaozuo, China

^cSchool of Energy and Mining Engineering,
China University of Mining and Technology, Beijing, China

Original scientific paper

<https://doi.org/10.2298/TSCI220812005Z>

Heat shock is a feasible means to break rock mass in engineering duo to the large additional thermal stress caused by thermal expansion. This paper established a coupled thermal transfer and rock deformation model based on the energy conservation and the elastic deformation theory of rock. In the model, the failure and damage of rock are judged according to the Drucker-Prager criterion. A finite element method of COMSOL Multiphysics to study the characteristics of temperature, stress distribution and damage zone on a rock surface is proposed. Results show that the failure of rock mass occurs at the cusps of the heater first duo to stress concentration and then grows at both sides of the heater greatly.

Key words: heat shock, thermal damage, thermo-mechanical model, numerical simulation

Introduction

The core of the traditional mechanical rock crushing technology mainly uses the rotation and impact of the drill bit to destroy the rock, which has a long history, mature technology and wide application [1]. However, for very hard rocks, especially in deep rock and mining engineering, the wear of tool severely limits the progress of the project [2]. The development and research of new rock breaking technologies has become a new subject in the field of geotechnical engineering. With the development of applied thermodynamics, some scholars have noticed the positive effect of heat shock on rock breaking. Domestic and foreign scholars have carried out loading and unloading tests [3]. For example, the thermal and mechanical interactions of rocks after the treatments of microwave irradiation [4, 5] and laser irradiation [6, 7] in the laboratory are explored, respectively.

External heating increases the temperature of rocks from the outside to the inside, or from inside to outside (microwave heating). The raise of rock temperature produces additional

*Corresponding author, e-mail: T.Teng@cumtb.edu.cn

thermal stress leading to thermal damage and failure. It is known that rock is a typical heterogeneous structure, which contains large and small holes and cracks [8], rock damage changes the mechanical properties and microstructure of rock [9]. Due to the different thermal expansion of each mineral component in rock after heated, cracks are formed between the cemented particles and further spread and develop in [10]. As a result of such changes in the internal microstructure of rock, the macroscopic physical mechanics of rock also changes, manifested as the elastic modulus, Poisson's ratio, compressive strength, and tensile strength all decrease [3]. For example, the coupled effects of thermal expansion, thermal fracturing, thermal damage, and thermal volatilization after heat shock were pointed in [11]. The evidences of long-term high temperature fluid-rock interactions in the serpentinized wehrlite were provided in [12].

In this paper, a fully coupled thermal-mechanical model for the analysis of temperature distribution and the damage of rock mass is established. Then, the COMSOL Multiphysics numerical simulation software is used to implement a numerical simulation work to study the effects of heat shock on rock. This research has positive significance for thermal breaking technologies in deep rock engineering.

A thermal-mechanical model

The volume expands when the temperature of rock mass increases, which is called thermal expansion. As the volume of the rock structure increases, the solid elements are subjected to higher levels of stress. The additional thermal stress has a great influence on the strength and stability of solid or rock structures, and may cause cracks in some components. These cracks can undermine the overall strength of the structure, leading to potential weakening and failures of rock mass.

Heat transfer equation

The generalized heat transfer equation is often expressed:

$$\rho C_p \frac{\partial T}{\partial t} + \nabla(-k\nabla T) + \rho C_p \mathbf{u}\nabla T - \tau : \mathbf{F} - \frac{T}{\rho} \left(\frac{\partial \rho}{\partial t} \right)_p \left(\frac{\partial p_a}{\partial t} + \mathbf{u}\nabla p_a \right) = Q \quad (1)$$

where the first term on the left means the accumulation of heat, the second term stands for the heat conduction, and the third term stands for the convective heat transfer of liquid. In this study, no convection is considered in the rock sample, thus $\rho C_p \mathbf{u}\nabla T = 0$. $\tau : \mathbf{F}$ is viscous heat of heat convection that also equals to 0 in this research; the fifth term on the left represents the pressure effect induced by the internal pore gas which is also ignored. The only term on the right, Q , is heat source or sink.

Therefore, the heat transfer equation can be simplified:

$$\rho C_p \frac{\partial T}{\partial t} + \nabla(-k\nabla T) = Q \quad (2)$$

where ρ is the density of rock mass and k is the thermal conductivity coefficient.

Here, eq. (2) is generalized by using the general operators in [13].

Elastic deformation of rock

This paper assumes that rocks are completely elastic materials, thus the deformation of rock is to be expressed by the constitutive equation of linear relation:

$$\mathbf{S} = \mathbf{S}_{ad} + \mathbf{C} : \boldsymbol{\varepsilon}_{el} \quad (3)$$

where S represents the stress, S_{ad} – the initial stress, C – the elastic modulus, and ε_{el} represents the elastic strain. The relationship between strain and displacement is:

$$\varepsilon_{el} = \frac{1}{2} [(\nabla u)^T + (\nabla u)] \quad (4)$$

Here, eq. (4) is one of the special cases reported in [14, 15].

According to the theory of elasticity, the general balance equation of stress in rock can be expressed:

$$\nabla S + F_v = 0 \quad (5)$$

where F_v is the additional body force in each element and ∇ stands for the Hamiltonian operator.

Thermal expansion usually takes the form from thermal strain:

$$S_T = C : \varepsilon_{th} = C \alpha_T \Delta T \quad (6)$$

where ε_{th} is thermal strain in x -, y - or z -direction, ΔT – the increment of temperature, and α_T means the thermal expansion coefficient for rock mass which can be divided into three components of α_{Tx} , α_{Ty} , α_{Tz} in x -, y - or z -direction if the anisotropy of thermal expansion is considered.

Thus, the effective stress S'_{ij} in variable thermal environment can be expressed:

$$S' = S + S_T \quad (7)$$

By substituting eqs. (6) and (7) into eq. (5), one can solve the elastic deformation and stress distribution of rock under variable temperature.

Rock failure criterion after heat shock

The Drucker-Prager criterion (D-P criterion in short) is used to evaluate the failure of rock mass in this work. It generally refers to a yield theory that considers the maximum shear stress, which also considers the effect of hydrostatic pressure:

$$f = \alpha I_1 + J_2^{1/2} - M^* \quad (8)$$

where

$$\alpha = \frac{\sin \varphi}{(9 + 3 \sin^2 \varphi)^{1/2}}, \quad M^* = \frac{3c \cdot \cos \varphi}{(9 + 3 \sin^2 \varphi)^{1/2}} \quad (9)$$

where c and φ are the cohesion and internal friction angle for rock, respectively. When the temperature of rock changes, the stress in eq. (8) must be revised by the effective stress. The mechanical parameters of rock mass might be revised as well.

Figure 1 is the curve evolution of rock state with variable internal friction angle after Drucker-Prager criterion. The compressive stress in the x -, y -, and z -directions are 0 MPa, 5 MPa, and 25 MPa, respectively. From fig. 1 and eq. (8), one can find that the rocks with larger values of internal friction angle and cohesion are easier to break after heat shock.

Numerical simulation method

Equations (2), (5), and (8) constitute a fully coupled thermal and mechanical model. In the following sections of this paper in, a numerical analysis based on the COMSOL Mul-

tip physics software is proposed meticulously to present the evolution of temperature and damage distribution in rock under heat shock.

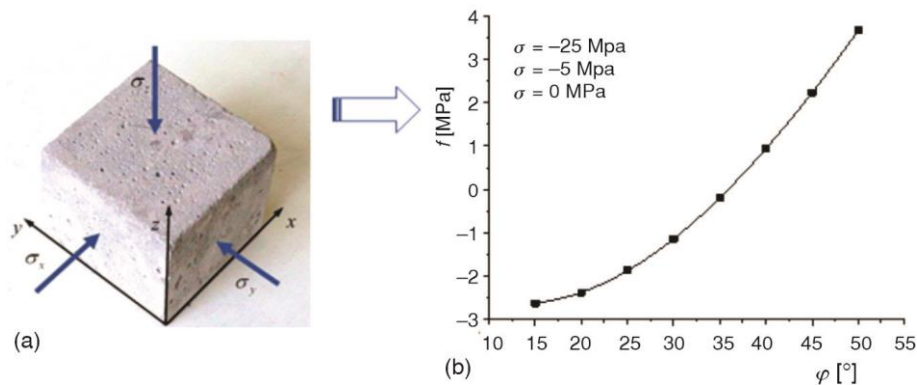


Figure 1. Curve of rock state after Drucker-Prager criterion;
(a) diagram of stressed rock and (b) calculated f with different ϕ

Establishment of rock face

In this paper, the 3-D rock mass under the in-situ stress conditions of the original work face is simplified into a 2-D plane stress rock face. The physical size of rock face is determined as 4 m in width and 4.8 m in height. For solid mechanical field, the initial stresses in the horizontal and vertical directions are 5 MPa and 20 MPa, respectively. As it is difficult to directly simulate rock mass with both in-situ rock stress with four-way constraint boundaries. The in-situ rock stress is firstly simulated here to realize the addition of initial stress, as shown in fig. 2(a). The simulated results are then added by the four-way roller support boundaries with the calculated distribution of stress in the solid mechanical field, fig. 2(b).

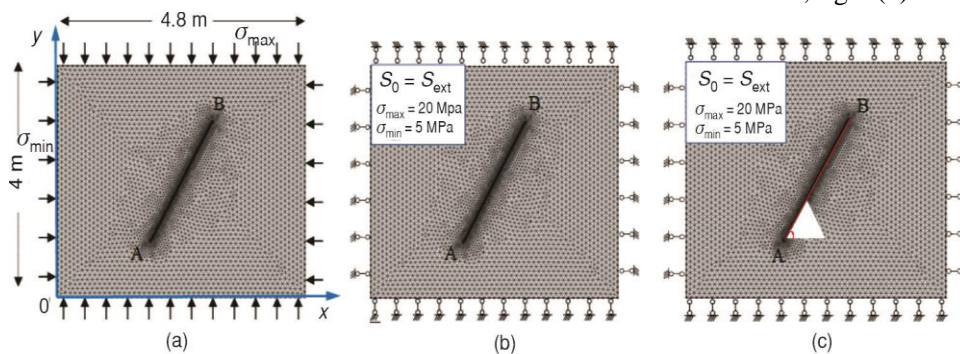


Figure 2. Establishment of numerical model

Conditions of heater

Figure 2 shows that a thermostatic heater AB that rotating an angle of α_1 with the coordinate x axis preset in the central position of the model. In the numerical work, the length and rotation angle of the heater is 2.5 m and 60° , respectively. The temperature of heater keeps 1200°C in variably. The initial temperature of the rock mass is 20°C . Physical and mechanical parameters that used in numerical simulation are given in tab. 1.

Table 1. Parameters for numerical model settings

Simulation parameters	Variable	Value	Unit
Modulus of elasticity	E	25	GPa
Poisson's ratio	ν	0.28	1
Density of rock	ρ	2600	kg/m ³
Thermal conductivity	k	2.73	W/mK
Heat capacity at constant pressure	C_p	963	J/kgK
Coefficient of thermal expansion	α_T	5×10^{-6}	1/K
Angle between the heater and the x -axis	α_l	0~90	°
The axial pressure	σ_{\max}	20	MPa
The confining pressure	σ_{\min}	5	MPa
Cohesion	c	27.2	MPa
Internal friction angle	φ	42	°

Results of the simulation

Temperature distribution on rock surface

Figure 3 is the distribution of temperature on rock surface after a heat shock time of 150 minutes. In the figure, an observation line CD is set in the direction perpendicular to the temperature heater. Heat transfers from the boundary of heater into the marginal area of rock mass. However, the temperature of the rock layer is not rising very fast due to the relatively large heat capacity. Figure 3 shows that affect distance of temperature is about 0.5 meter after 150 minutes on both sides of the heater boundaries. Besides, the decreasing rate of rock temperature slows down gradually with the distance from the heater, forming a peak-like region of high temperature. This is consistent with the heat conduction equation mentioned earlier in this paper.

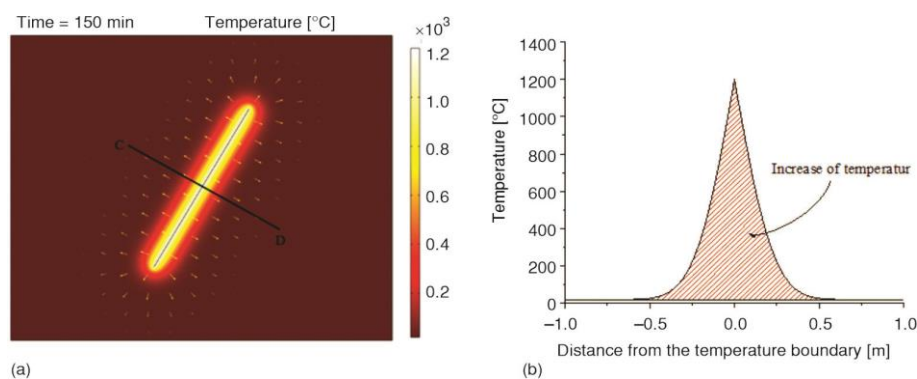


Figure 3. Distribution of temperature after 150 min; (a) temperature contour map and (b) temperature in CD direction

Evolution of damage zone after heat shock

According to the Drucker-Prager criterion, rocks break down when the stress is high enough. To analyze the final performance of rock breaking by the means of heat shock, a variable of the proportion of damage zone in the whole rock face is defined:

$$b = \frac{A_1}{A_0} \quad (10)$$

where A_0 is the total area of the 2-D geometry and A_1 is the area of damaged rock. From the introduced modelling process, we take $A_0 = 19.2 \text{ m}^2$.

Figure 4 shows the evolution of the damage zone on the surface of rock mass after different heat shock times of 10, 20, 30, and 40 minutes. At the time of 10 and 20 minutes, the damage of rock mainly occurs at the cusps of the heater which is greatly dominated by the concentration of stress. When the heating time reaches to 30 or 40 minutes, the damage at the sides of the heater increases obviously due to the larger additional thermal stress caused thermal expansion. On the whole, the damage zone extends from the periphery of the heater to the edge of the model. As a result, the proportion of damaged area increases from 15% to 39.8% when the heating time increases from 10 to 40 minutes.

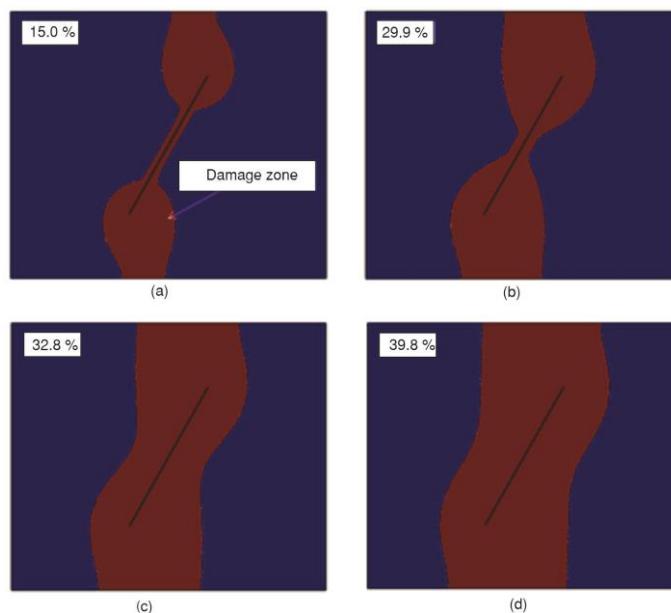


Figure 4. Evolution of damage zone on rock surface; (a) heating 10 min, (b) heating 20 min, (c) heating 30 min, and (d) heating 40 min

Proportion of damage zone with different angle of heater

For a particular engineering project, the mechanical properties and the distribution of their-situ stress in rock mass are often stratigraphically determined. Based on the prerequisites, a suitable arrangement angle of thermal heater with the co-ordinate x axis is significantly to be well designed and optimized to achieve the best breaking result of rock.

Figure 5 discusses the proportion of damage zone in rock face with different angle of α_1 at the heating time of 40 minutes. Ten different

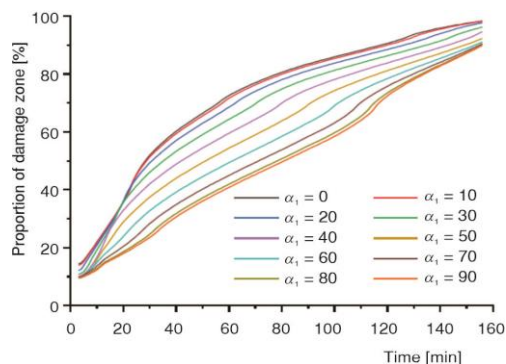


Figure 5. Proportion of damage zone in rock face with different angle

angles varying from zero to 90° are chosen to compare the final performance of damage after heat shock. It can be seen from fig. 5 that the growth rate of the damage zone is tapering off with the heating time. Besides, the damage zone has the largest proportion in the total area of the working face when the heater is arranged perpendicular to the direction of maximum principal stress which is parallel to the long side of the working face is the numerical simulation.

Conclusion

In this work, a coupled thermal transfer and rock deformation model based on the energy conservation and the elastic deformation theory was established. The Drucker-Prager criterion is used to judge the thermal damage of rock. Then, a finite element method of COMSOL Multiphysics to analyze the characteristics of temperature distribution and damage zone on a rock surface is proposed. Numerical study on the effects of heat shock with constant temperature condition on damage characteristics and the evolution of influence range is studied. Temperature of rock rises relatively slow due to the large heat capacity, but higher temperature causes larger thermal stress and significant failure of rock. The damage zone formed on the surface of rock mass extends from the periphery of the heater to the edge of the model. But the growth rate of the damage zone tapers off with heating time. The damage zone has the largest proportion in the total area of the working face when the heater is arranged perpendicular to the direction of maximum principal stress which is parallel to the long side of the working face.

Acknowledgments

The authors are grateful to the financial support from National Natural Science Foundation of China (52004285, U1910206), the Open Fund of the State Key Laboratory Cultivation Base for Gas Geology and Gas Control (Henan Polytechnic University) (WS2021A03), the Fundamental Research Funds for the Central Universities (2022JCCXXNY06) and National Training Program of Innovation and Entrepreneurship for Undergraduates (202111004, 202211033).

Nomenclature

C_p	– heat capacity of rock, [Jkg ⁻¹ K ⁻¹]	S	– stress, [MPa]
I_1	– first stress tensor invariant, [MPa]	T	– temperature, [°C]
J_2	– second invariant of stress deviator, [MPa]	t	– time coordinate, [s]

References

- [1] Deng, R., et al., Simulation and Experimental Research of Laser Scanning Breaking Granite, *Optics Communications*, 502 (2022), Jan., 127403
- [2] Jakobsen, P. D., et al., Review and Assessment of the NTNU/SINTEF Soil Abrasion Test (SAT™) for Determination of Abrasiveness of Soil and Soft Ground, *Tunnelling and Underground Space Technology*, 37 (2013), Aug., pp. 107-114
- [3] Kang, F. C., et al., Experimental Study on the Physical and Mechanical Variations of Hot Granite under Different Cooling Treatments, *Renewable Energy*, 179 (2021), Jul., pp. 1316-1328
- [4] Lu, G. M., et al., The Influence of Microwave Irradiation on Thermal Properties of Main Rock-Forming Minerals, *Applied Thermal Engineering*, 112 (2017), Feb., pp. 1523-1532
- [5] Hartlieb, P., et al., Reaction of Different Rock Types to Low-Power (3.2 Kw) Microwave Irradiation in a Multimode Cavity, *Minerals Engineering*, 118 (2018), Mar., pp. 37-51
- [6] Li, X., et al., Effect of Microwave Irradiation on Dynamic Mode-I Fracture Parameters of Barre Granite, *Engineering Fracture Mechanics*, 224 (2020), Feb., 106748
- [7] Buckstegge, F., et al., Advanced Rock Drilling Technologies Using High Laser Power, *Physics Procedia*, 83 (2016), Sept., pp. 336-343

- [8] Homand, F., *et al.*, Thermally Induced Microcracking in Granites: Characterization and Analysis, *International Journal of Rock Mechanics and Mining Sciences & Geomechanics Abstracts*, 26 (1989), Mar., pp. 125-134
- [9] Morrow, C., *et al.*, Permeability of Granite in a Temperature Gradient, *Journal of Geophysical Research*, 86 (1981), Apr., pp. 3002-3008
- [10] Sirdesai, N. N., *et al.*, Effects of Thermal Treatment on Physico-Morphological Properties of Indian Fine-Grained Sandstone, *Bulletin of Engineering Geology and the Environment*, 78 (2019), Mar., pp. 883–897
- [11] Teng, T., *et al.*, Evaluation Criterion and Index for the Efficiency of Thermal Stimulation to Dual Coal Permeability, *Journal of Natural Gas Science and Engineering*, 68 (2019), Aug., 102899
- [12] Tushar, M. C., *et al.*, High Temperature Fluid-Rock Interaction Recorded in a Serpentinized Wehrlite from Eastern Singhbhum Craton, India: Evidence from Mineralogy, Geochemistry and in Situ Trace Elements of Clinopyroxene, *Lithos*, 404-405 (2021), Dec., 106498
- [13] Yang, X. J., *et al.*, A New Scaling Law Heat Conduction Problem Associated with the Korcak Scaling Law, *Thermal Science*, 26 (2022), 2A, pp. 1047-1059
- [14] Yang, X. J., *et al.*, On the Theory of the Fractal Scaling-Law Elasticity. *Meccanica*, 57 (2022), 4, pp. 943-955
- [15] Yang, X. J., An Insight on the Fractal Power Law Flow: From a Hausdorff Vector Calculus Perspective. *Fractals*, 30 (2022), 3, ID 2250054